**Rare Metal Materials and Engineering**
Volume 49, Issue 9, September 2020
Available online at www.rmme.ac.cn

Science Press

**Cite this article as:** Rare Metal Materials and Engineering, 2020, 49(9): 2966-2972.

ARTICLE

# Microstructure Simulation of ZL201 Aluminum Alloy Auxiliary Frame in Solidification Process

**Chen Junyu[1], Qiu Zhesheng[2], Li Jiaqi[2], Yan Jikang[1], Zhao Yanbo[2]**

*[1] Kunming University of Science and Technology, Kunming 650093, China; [2] Yunnan Aluminium Co., Ltd, Kunming 650502, China*

**Abstract:** The solidification process and microstructure of ZL201 aluminum alloy auxiliary frame were simulated by Cellular Automation (CA) method, and the temperature field and microstructure simulation (CAFE) field were established. According to the solid and liquid phase lines of ZL201 aluminum alloy, six different nucleating surfaces were determined. The simulation results of temperature field show that the nucleation rate and growth rate can be controlled in the most suitable range by oil cooling. The nucleation rate is 1/276 s·cm$^3$ and growth rate is 65.2 μm/s. The calculation results of thermodynamic phase diagram show that in the formation process of $Al_3Ti$ phase, it absorbs covalent electrons from surrounding aluminum atoms. With the increasing of titanium content, the precipitation temperature of $Al_3Ti$ increases. In addition, the content of $Al_3Ti$ has increased from 0.144 mol% to 0.698 mol%, and the effect of grain refinement becomes more and more obvious. Through the simulation of the microstructure of ZL201 aluminum alloy auxiliary frame, the corresponding <100> polar diagram and the experimental metallographic structure, it is shown that the change of Ti content has a significant impact on the grain refinement effect of ZL201 aluminum alloy auxiliary frame microstructure. With the increasing of titanium content, the new phase $Al_3Ti$ promotes grain refinement and composition uniformity. It can be seen from the simulated polar diagram of <100> that the increase of Ti content is conducive to the preferential orientation of grains, and the grain refinement is achieved by slowing down the competition among grains. The results of simulation are basically consistent with the metallographic structure obtained by experiment.

**Key words:** ZL201 aluminum alloy; analog simulation; solidification process; auxiliary frame

In recent years, the lightweight automobile has become the trend of development, which is an effective measure to deal with the energy and environmental problems caused by the rapid growth of car ownership[1]. The advantages of ZL201 aluminum alloy include low density, good formability and excellent corrosion resistance, which has become an important way to realize automobile lightweight[2]. ZL201 aluminum alloy has been widely used in automobile body, chassis and powertrain. In particular, it is applied to the auxiliary frame in the chassis[3]. Fig.1 shows that the auxiliary frame of U-shaped structure[4]. In order to realize the lightweight of auxiliary frame, the requirement of aluminum alloy casting is also raised[5]. It is mainly reflected in high forming precision, the microstructure of small size, uniform composition, and excellent macro performance. Simulation analysis is necessary to control the solidification process[6].

The solidification process is a very important stage in material processing and preparation. During the forming process, most metals and metal alloys have solidification processes[7]. The microstructure obtained by solidification process will directly affect the macro-properties of materials[8]. The most essential factors determining the mechanical properties of materials are the morphology, size, orientation and distribution of the internal grains of castings[9]. Therefore, the change of solidification structure will have a great impact on the mechanical properties of castings, and the control of solidification structure is the key to obtain

Received date: September 25, 2019
Foundation item: National Natural Science Foundation of China (51362017); Major Science and Technology Project of Yunnan Province-Major Project of New Materials (2018ZE005)
Corresponding author: Yan Jikang, Ph. D., Professor, Faculty of Materials Science and Engineering, Kunming University of Science and Technology, Kunming 650093, P. R. China, E-mail: scyjk@qq.com

high quality casting[10]. The solidification process involves a series of complex physical and chemical changes. The macroscopic properties show that the solidification is accompanied by heat transfer, mass transfer and flow[11]. The microscopic properties show that the solidification is a dynamic process of nucleation and growth[12]. Due to the complex influence between macro and micro, the theoretical study and mathematical analysis of solidified microstructure are very difficult[13]. In recent years, with the development of experimental technology, the establishment of computer simulation model greatly reduces the problem involving time and production cycle[14]. The research method of microscopic simulation is mainly to the grain size and morphology of solidified microstructure are predicted by establishing the dynamic model of nucleation growth process[7]. Therefore, in the microstructure simulation of solidification process, it is not only necessary to calculate the macroscopic temperature field and now field, but also to simulate the grain nucleation and growth process[15]. The authors hold that the blending of different models and the coupling of models with macro-field simulation will be the future tendency for the simulation of microstructure during solidification[16]. In the study of microstructure simulation, Cellular Automation (CA) have simulated quantitatively the effect of supercooling degree and solute distribution on the solidification process. CA can describe the formation process of free dendrites and columnar crystals and the transformation process of columnar crystals and equiaxed crystals[17].

In this work, the cooling and solidification process of ZL201 aluminum alloy auxiliary frame were simulated by CA method Fig.1 is structural drawing of the auxiliary frame. The temperature field and CAFE field were established. Firstly, the nucleation surface was determined by the temperature field, and then the influence of Ti content on microstructure was analyzed. When the content of Ti is 0.45 mol% and 0.75 mol%, it plays an obvious role in grain refinement. Finally, combined with the microstructure of ZL201 aluminum alloy auxiliary frame and corresponding <100> orientation pole figure, the refinement effect of Ti was further verified.


Fig.1 Structural drawing of the auxiliary frame

1-steering bracket, 2-mount bracket, 3-steering engine, 4-shock absorber, 5-spring, 6-tire, 7-steering knuckle, 8-stabilizer rod, 9-auxiliary frame, 10-stabilizer bar, 11-control arm

## 1 Model Establishment and Parameters Determination

### 1.1 Macroscopic and microscopic meshing models

In the simulation process, surface mesh and volume mesh are divided. In addition, the generation of grid includes macroscopic temperature field and microstructure simulation (CAFE)[18]. Equilateral triangle is used to divide the grid cells. The grid size of ZL201 auxiliary frame is 20 mm and the sample is 0.3 mm. In order to analyze thoroughly the microstructure affected by different Cu content, the nucleation surface was sampled and analyzed. The sample is a cylinder with a diameter of 5 mm and a height of 10 mm (as see in Fig.2).

In order to accurately simulate the microstructure of grain growth and size, the grid needs to be continuously optimized. The particle of nucleation grows in subdivided mesh. The mesh division should not only ensure the number of nucleated particles in the mesh, but also ensure that the growth of grains cannot exceed the range of a cell.

### 1.2 Calculation of various thermophysical parameters

The ZL201 auxiliary frame was manufactured by low-pressure die casting (LPDC) method. The composition of alloy elements is shown in Table 1. We only changed the content of Cu in the three schemes. The cooling and solidification process of ZL201 auxiliary frame was simulated by CA method. The temperature of mold was set to 350 ºC, and the casting was 750 ºC. In the process of simulating macroscopic temperature field and microstructure, the accuracy of thermophysical parameters would directly affect the results of calculation and simulation. In the model ZL201 auxiliary frame, the solid phase fraction calculation of intracellular grains is based on Scheil equation[19].

$$C_s = k_e C_0 (1 - f_s)^{k_e - 1} \quad (1)$$

Where $k_e$ is the effective solute solidification coefficient; $C_0$ is initial composition; $f_s$ is frequency; $C_s$ is solute segregation of solid phase.

In the microstructure simulation, the growth coefficient directly determines the growth rate of dendrites. The coefficient of growth can be expressed as follows[20]:

$$\alpha = [\frac{-\rho}{(mc_0)(1-k)^2 \cdot 2\Gamma k} + \frac{mc_0}{(mc_0)(1-k)D}] \cdot \frac{D^2}{\pi^2 \Gamma} \quad (2)$$

$$\beta = \frac{D^2}{\pi \Gamma} \cdot \frac{1}{(mc_0)(1-k)^2 D} \quad (3)$$

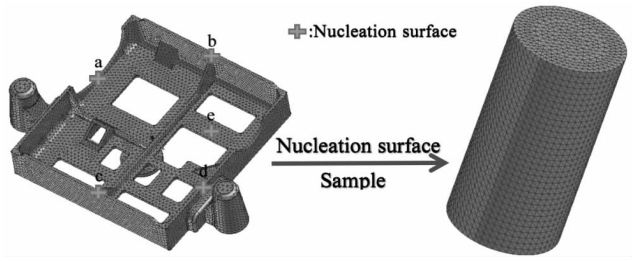


Fig.2 Grid cells divided by temperature field and CAFE field

$m$ is liquid phase slope; $c_0$ is alloy composition; $\Gamma$ is Gibbs-Thompson parameter; $D$ is liquid diffusion coefficient; $k$ is equilibrium solute partition coefficient; $\alpha$ is the first level growth coefficient; $\beta$ is the second level growth coefficient. The microstructure simulation required for the values of thermophysical parameters and growth coefficients are listed in Table 2.

## 2 Simulation Result and Analysis

### 2.1 Analysis of cooling and solidification process

Setting the heat transfer coefficient between the casting and the mold as $h$=300. The temperature distribution of castings during solidification was analyzed under the three different conditions of oil cooling, air cooling and slow cooling. The cooling and solidification process of the temperature field distribution of ZL201 auxiliary frame is shown in Fig.3.

The start time was calculated after the completion of filling. Initial temperature field was obtained by steady-state analysis at 0.01 s. The initial temperature of the casting is 750 ºC. Contacting between castings and molds results in a strong heat exchange. It makes the temperature of the inner surface part of the casting in contact with mold rise rapidly from 350 ºC to 720 ºC, and the temperature of most parts of the mold is still the initial temperature of 350 ºC. Section A is the first to reach the liquidus temperature (652~660.2 ºC), and it begins to precipitate the solid phase at stage 1. In the stage 2, the temperature of the most parts of casting begins to drop. Since the cooling condition is superior, the temperature of the casting edge drops, and it has fallen to below 650 ºC. The results show that the most parts of liquid aluminum alloy begin to solidify, which accords with the basic physical process of heat conduction. When the process continues to stage 4, the casting center and section B are still the liquid, and other positions have dropped below the temperature of the solid phase line (540 ºC). At this time, the heat dissipation conditions of the casting edge part is supreme. This stage completes the transformation from liquid state to solid state, and the phase transition zone begins to spread to the surface of the casting. When solidification reaches stage 6, the temperature of the casting center drops to 209 ºC, and the outside temperature drops to 195 ºC. Since the internal and external temperature difference is less than 15 ºC, the rate of descent of the casting temperature becomes slow. The heat exchange process is basically complete until it cools to room temperature.

### 2.2 Microstructure simulation analysis

Fig.4, Fig.5 and Fig.6 show simulated microstructure of the ZL201 auxiliary frame with different Ti contents. The Ti contents are 0.15 mol%, 0.45 mol% and 0.75 mol%, respectively. The microstructure was simulated in three different cooling modes. Cooling methods include water cooling (FilmCo=10, $T$=25 ºC), oil cooling (FilmCo=1500, $T$=160 ºC) and slow cooling (FilmCo=500, $T$=25 ºC). Different colors represent grains of different orientations. According to the simulation results of the temperature field, a total of six nucleation surfaces were selected. In the actual production, mold wall, mold temperature, alloy composition, process and so on will affect the result of nucleation. It can be seen that the auxiliary frame casting is prepared by water cooling, and the structure uniformity is poor. The grain size of ZL201 aluminum alloy casting depends on nucleation rate and growth rate[21]. Grain refinement can only be achieved by increasing nucleation rate and decreasing growth rate. The cooling velocity of oil is the lowest in the three cooling methods. With the increase of the cooling rate, the nucleation rate and the growth rate of the crystal are faster, which accelerates the crystallization process. However, when the cooling velocity reaches a certain value, the crystallization process will slow down. This is because the diffusion ability of the atom is weakened. The nucleation rate and growth rate can be well controlled in the most suitable range by oil cooling. The nucleation rate is 1/276 s·cm$^3$ and growth rate is 65.2 μm/s. The microstructure models show that the final shape of the grains of the casting is dendritic at the thin wall (section C). It shows that the

**Table 1 Element composition of ZL201 auxiliary frame (mol%)**

| Elementary composition | Cu | Mn | Fe | Ti | Al |
|---|---|---|---|---|---|
| 1 | 5.0 | 0.8 | 0.1 | 0.15 | Bal. |
| 2 | 5.0 | 0.8 | 0.1 | 0.45 | Bal. |
| 3 | 5.0 | 0.8 | 0.1 | 0.75 | Bal. |

**Table 2 Simulation thermophysical parameters of ZL201 auxiliary frame**

| Parameter | Elementary composition | | |
|---|---|---|---|
| | 1 | 2 | 3 |
| Liquidus temperature, $k_L$/K | 652.0 | 658.3 | 660.2 |
| Solidus temperature, $k_S$/K | 548.3 | 550.6 | 554.3 |
| Gibbs-Thompson, $\Gamma$ | $1\times10^{-7}$ | $1\times10^{-7}$ | $1\times10^{-7}$ |
| Coefficient of growth ($\alpha$, $\beta$) | $4.82\times10^{-7}(\alpha)$ | $4.75\times10^{-7}(\alpha)$ | $4.45\times10^{-7}(\alpha)$ |
| | $4.98\times10^{-6}(\beta)$ | $3.74\times10^{-6}(\beta)$ | $2.36\times10^{-6}(\beta)$ |
| Maximum nucleation density, $n_{max}$ /m$^3$ | $1\times10^9$ | $1\times10^9$ | $1\times10^9$ |
| Average nucleation and sub-cooling, $\Delta T_n$/K | 0.5 | 0.5 | 0.5 |
| Standard curvature sub-cooling, $\Delta T_\partial$/K | 0.1 | 0.1 | 0.1 |

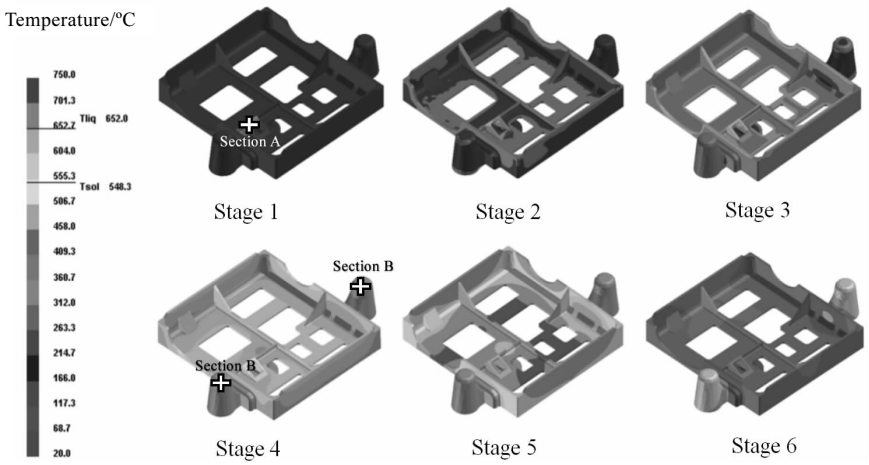


Fig.3 Temperature field of the cooling and solidification stages of ZL201 auxiliary frame

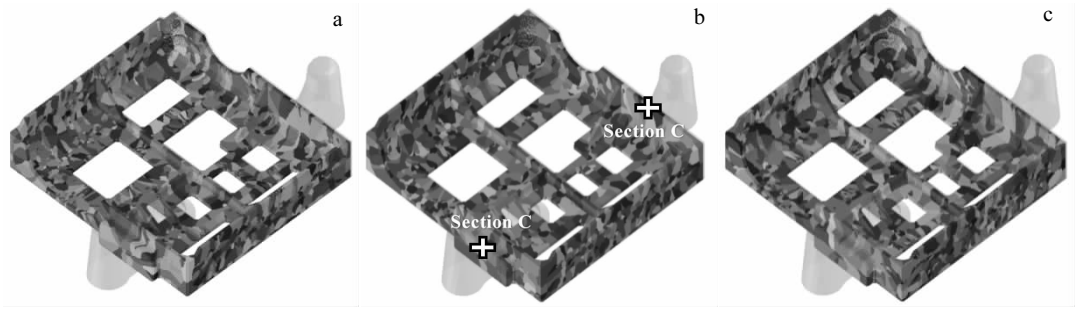


Fig.4 Simulated microstructure of ZL201 with 0.15 mol%Ti: (a) FilmCo=10, *T*=25 ºC; (b) FilmCo=1500, *T*=160 ºC; (c) FilmCo=500, *T*=25 ºC

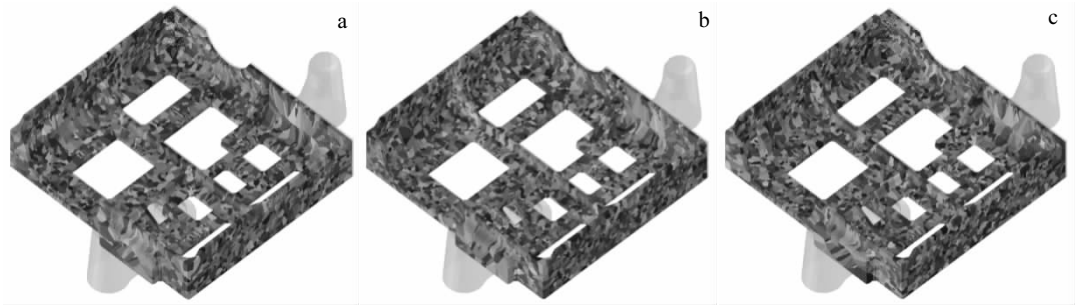


Fig.5 Simulated microstructure of ZL201 with 0.45 mol%Ti: (a) FilmCo=10, *T*=25 ºC; (b) FilmCo=1500, *T*=160 ºC; (c) FilmCo=500, *T*=25 ºC

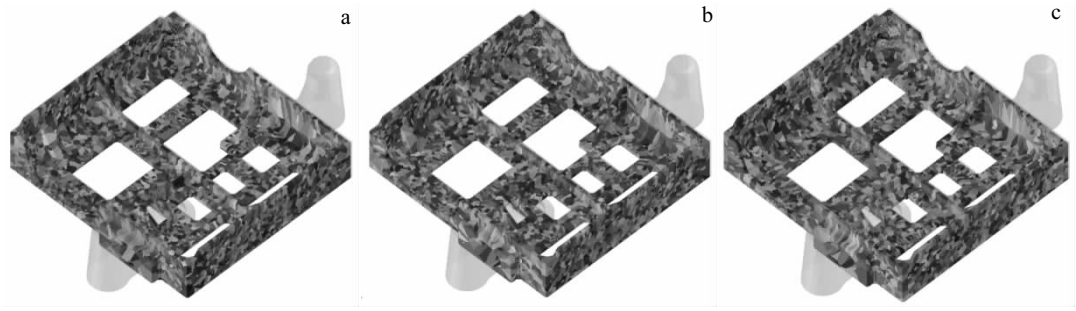


Fig.6 Simulated microstructure of ZL201 with 0.75 mol%Ti: (a) FilmCo=10, *T*=25 ºC; (b) FilmCo=1500, *T*=160 ºC; (c) FilmCo=500, *T*=25 ºC

grain growth trend is consistent with the direction of temperature gradient at the section C. In addition, with the increase of Ti content, the microstructure is more uniform and the grain is refined. The phase diagrams of the different Ti content were calculated by the principle of thermodynamics as shown in Fig.7. It predicts that when Ti content is 0.45 mol% and 0.75 mol%, the new phase $Al_3Ti$-Mn is found in the phase diagram. It predicates that the appearance of new phase $Al_3Ti$-Mn is beneficial to improve the homogeneity of microstructure and refine grain.

### 2.3 Thermodynamic phase diagram calculation

At the beginning of solidification, a layer of tiny and randomly oriented equiaxed crystals is found at the bottom of the sample. As the solidification time continues, in other words, with the increase of the distance of sample nucleation surface, the number of grains decreases gradually at the cross section, and the grain size increases gradually. When the Ti content is more than 0.15mol%, the new phase $Al_3Ti$-Mn is found in Fig.7. It results in more uniform microstructure and finer grain size. In Zl201 aluminum alloy, the crystal reaction of $Al_3Ti$ phase is as follows[22]:

$$L+Al_3Ti \rightarrow \alpha(Al) \quad (4)$$

Peritectic reaction can promote grain refinement. $\alpha$-Al nucleation is promoted by the peritectic reaction between $Al_3Ti$ and liquid alloy. When Ti is added to ZL201 aluminum alloy, $Al_3Ti$ phase will be formed. Al and $Al_3Ti$ form a coherency relation. The $\alpha$-Al can grow around $Al_3Ti$-Mn. It indicates that during the formation of $Al_3Ti$ phase, it absorbs covalent electrons from surrounding Al atoms. At this time, $Al_3Ti$ is negatively charged, while surrounding Al is positively charged due to the loss of covalent electrons. Therefore, it is easier for Al to grow with $Al_3Ti$ as crystal nucleus, and the grain is further refined. According to the thermodynamic phase diagram, when the Ti content is 0.15 mol%, the precipitation temperature of $Al_3Ti$ is 682 ºC. At this time, the effect of grain refinement is not obvious. The increase of Ti content increases the precipitation temperature of $Al_3Ti$. In addition, it also increases the $Al_3Ti$ content from 0.144 mol% to 0.698 mol%. The effect of grain refinement is more and more obvious. The addition of Mn promotes the reaction variable of $Al_3Ti$ peritectic reaction and the solubility of titanium. As a result, the peritectic point is shifted to the low content of titanium, and the Mn can further refine grains.

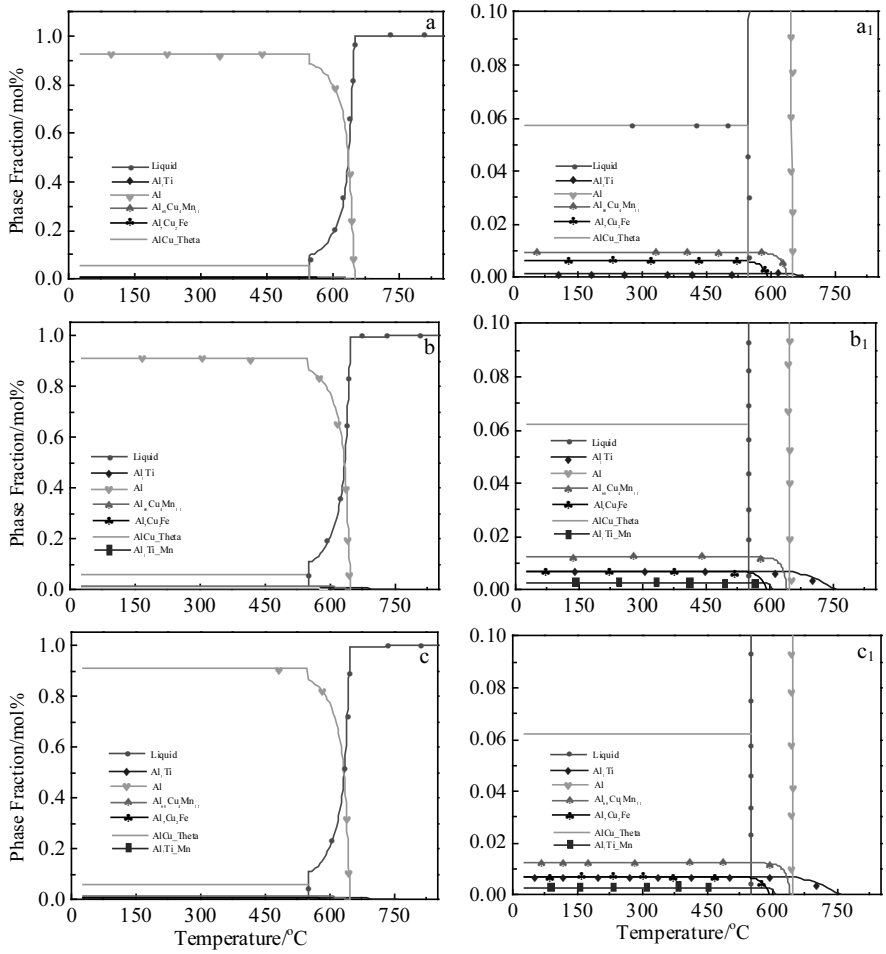


Fig.7 ZL201 phase diagrams with different Ti content calculated by the principle of thermodynamics: (a) ZL201-0.15 mol%Ti, (b) ZL201-0.45 mol%Ti, and (c) ZL201-0.75 mol%Ti

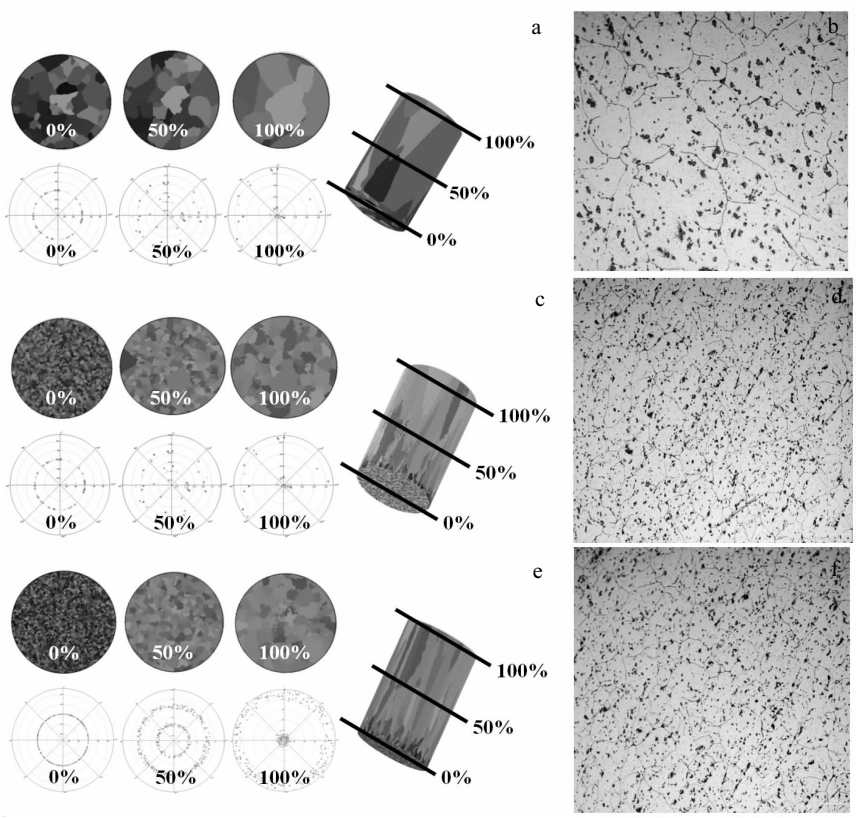


Fig.8 Simulating the microstructures of ZL201 aluminum alloy auxiliary frame and corresponding <100> orientation pole figure (a, c, e), and the metallographs at 100 mol% section (b, d, f): (a, b) 0.15 mol% Ti, (c, d) 0.45 mol% Ti, and (e, f ) 0.75 mol%Ti

### 2.4 <100> orientated simulation analysis

To further analyze the simulation results, Fig.8 shows that the nucleated surface is sampled, and it is a cylinder with a height of 10 mm and a diameter of 5 mm. Start at the bottom of the sample, the cross section are made at the bottom, the middle and the top of the sample. The grain growth simulation diagram of cross each section and the corresponding <100> orientation pole figure are shown in Fig.8. It can be seen that at the beginning of solidification, a layer of fine and randomly oriented equiaxed crystals is found at the bottom of the sample. As the temperature continues to drop, polarization appears in the grains and they begin to grow preferentially at two opposite directions. The phenomena are more obvious with the increase of Ti content. Because the growth of randomly oriented equiaxed crystals is more competitive at the bottom of the sample. As the sample continues to solidify, the number of grains on the cross section gradually decreases. When the Ti contents are 0.45mol% and 0.75mol%, competitive growth of grains becomes slow. Finally, the purpose of grain refinement is achieved[23].

The metallographic structure of ZL201 aluminum alloy auxiliary frame indicates that the grain size is the largest when Ti content is 0.15mol%, whose structure is dendritic crystal and whose shape is schistose. When Ti content continues to increase, the grains are obviously refined. The most are fine equiaxial crystals. In the solidification process, the growth of dendrites has a preferred orientation. Only those grains that are consistent with the direction of the temperature gradient will grow, while other grains that deviate from the direction of the temperature gradient will be gradually eliminated by the preferential orientation of grains in the growth process. In the solidification process of the casting of auxiliary frame, the temperature gradient is the largest and the heat dissipation is the fastest on the *z*-axis. It shows that the growth rate of grains is the highest, and the growth of grains is restricted by the adjacent grains. It makes them grow up as fast as possible and reach other grain fronts, which hinders the growth of other oriented grains. In this research, the results of simulation are consistent with this manuscript[24,25].

## 3 Conclusions

1) The temperature fields indicate that during the solidification process, the temperature of the center of the casting is high, and the surrounding is relatively low. The boundary area in contact with the casting mold is the first to solidify. The temperature drops from the center to the outside in the ZL201 auxiliary frame casting. Through the oil cooling can well control nucleation rate and growth rate within the most

suitable range.

2) The thermodynamic phase diagram indicates during the formation of $Al_3Ti$ phase, it absorbs covalent electrons from surrounding Al atoms. The increase of Ti content increases the precipitation temperature of $Al_3Ti$. In addition, it also increases the $Al_3Ti$ content from 0.144 mol% to 0.698 mol%. The effect of grain refinement is more and more obvious.

3) The microstructure simulation of ZL201 aluminum alloy auxiliary frame, corresponding <100> orientation pole figure and metallographic structure show that the change of Ti content has a significant effect on the microstructure of ZL201 auxiliary frame. The increase of Ti content is beneficial to the preferred orientation of grains. The aim of grain refinement is achieved by slowing down the competitive growth of grains.

## References


1 Kim H C, Wallington T J, Sullivan J L *et al*. *Life Cycle Assessment*[J], 2019, 24(3): 397

2 Jing L, Tian L, Ping W. *Advanced Materials Research*[J], 2009, 79-82(8): 1423

3 Yong L, Duan X, Chi X *et al*. *Automobile Technology*[J], 2013, 12(9): 323

4 Liu D. *Automobile Technology*[J], 1995, 1(8): 24

5 Kang Q, Mao X Y, Lin J *et al*. *Advanced Materials Research*[J], 2013, 816-817(9): 255

6 Rashidi E, Najati A, Osgooei E. *Dynamical Sampling: Mixed Frame Operators, Representations and Perturbations*[J], 2019, 1(4): 121

7 Lu Yuzhang, Xiong Ying, Peng Jianqiang *et al*. *Journal of Materials Engineering*[J], 2018, 46(1): 8

8 Mirosław Seredyński, Battaglioli S, Robin P Mooney *et al*. *International Journal of Numerical Methods for Heat & Fluid Flow*[J], 2017, 27(5): 23

9 Zou J, Zhai Q J, Liu F Y *et al*. *Metals & Materials International*[J], 2018(7): 1

10 Xie M G, Zhu C A. *China Foundry*[J], 2017, 14(3): 176

11 Wu B, Jiang A L, Lu H *et al*. *Materials Science Forum*[J], 2018, 913(2): 212

12 Zou Q, Ning H, Shen Z *et al*. *Separation & Purification Technology*[J], 2018, 207(4): 151

13 Liu S, Fang Z W, Li L X. *IOP Conference Series Materials Science and Engineering*[J], 2018, 359(12): 1757

14 Li Z, Sheikholeslami M, Shafee A *et al*. *Journal of Molecular Liquids*[J], 2018, 266(9): 181

15 Gao T, Li Z Q, Zhang Y X *et al*. *Acta Metallurgica Sinica*[J], 2018, 31(1): 48

16 Nagarajan S G, Anbu G, Srinivasan M *et al*. *Silicon*[J], 2018(6): 1

17 Zhou D, Hu J, Gao X *et al*. *International Journal of Modern Physics B*[J], 2019, 33(8): 17

18 Pouraliakbar H, Jandaghi M R, Khalaj G. *Materials & Design*[J], 2019, 124(15):34

19 Yu Yingxia, He Bolin, Qi Qingyan. *Journal of Computational and Theoretical Nanoscience*[J], 2012, 9(9): 1214

20 Bu X B, Li L X, Zhu B W *et al*. *Journal of Materials Engineering & Performance*[J], 2013, 22(9): 2451

21 Wu I W, Chiang A, Fuse M *et al*. *Journal of Applied Physics*[J], 1989, 65(10): 4036

22 Maxwell I, Hellawell A. *Acta Metallurgica*[J], 1975, 23(8): 901

23 Sato H, Ota K, Watanabe Y *et al*. *Materials Science Forum*[J], 2006, 519-521(1): 1859

24 Nikulin, Kipelova, Malopheyev *et al*. *Acta Materialia*[J], 2012, 60(2): 487

25 Zhi L, Xing W M, Yong W *et al*. *Chinese Journal of Nonferrous Metals*[J], 2016, 12(6): 56 (in Chinese)


# ZL201 铝合金副车架凝固过程的微观组织模拟


陈俊宇[1]，邱哲生[2]，李家奇[2]，严继康[1]，赵艳波[2]

(1. 昆明理工大学，云南 昆明 650093)

(2. 云南铝业有限公司，云南 昆明 650502)



**摘　要：**采用元胞自动化(CA)方法对 ZL201 铝合金副车架的凝固过程和显微组织进行了模拟，建立了温度场和组织模拟场（CAFE）。对于面、体网格的划分，根据 ZL201 铝合金的固相线和液相线分别确定了 6 种不同的形核面。温度场的凝固过程模拟结果表明通过油冷可以很好地控制形核率和生长速率在最合适的范围内，形核率为 1/276 s·cm$^3$，生长速率为 65.2 μm/s。通过热力学相图的计算结果表明 $Al_3Ti$ 相的形成过程，它从周围的铝原子中吸收共价电子。随着钛含量的增加，$Al_3Ti$ 的析出温度升高。此外，$Al_3Ti$ 的含量也从 0.144 mol%提高到 0.698 mol%，晶粒细化的效果也随之越来越明显。通过对 ZL201 铝合金副车架的微观组织、对应的<100>取向极图和金相组织的模拟和实验对照，表明 Ti 含量的变化对 ZL201 铝合金副车架的微观组织的晶粒细化效果有显著影响。随着钛含量的增加，新相 $Al_3Ti$ 促进了晶粒细化和组成的均匀性。从模拟的<100>极图可知，Ti 含量的增加有利于晶粒的择优取向，而且晶粒细化的方式是通过减缓晶粒之间的生长竞争性来实现的。模拟的结果与实验得到的金相组织基本一致。



**关键词：**ZL201铝合金；模拟仿真；凝固过程；副车架



作者简介：陈俊宇，男，1994 年生，硕士，昆明理工大学材料科学与工程学院，云南 昆明 650093，E-mail: 754271418@qq.com